REPORT No. 487

AN AERODYNAMIC ANALYSIS OF THE AUTOGIRO ROTOR WITH A COMPARISON BETWEEN CALCULATED AND EXPERIMENTAL RESULTS

By John B. Wheatley

SUMMARY

An extension of the autogiro theory of Glauert and Lock is here presented in which the influence of a pitch varying with the blade radius is evaluated and methods of approximating the effect of blade tip losses and the influence of reversed velocities on the retreating blades are developed. The resulting equations have been applied to determine the characteristics of a PCA-2 autogiro rotor. A comparison of calculated and experimental results showed that most of the rotor characteristics could be calculated with reasonable accuracy, and that the type of induced flow assumed has a secondary effect upon the net rotor forces, although the flapping motion is influenced appreciably. An approximate evaluation of the effect of parasite drag on the rotor blades established the importance on including this factor in the analysis.

INTRODUCTION

The aerodynamic analysis of the autogiro rotor has been the subject of several studies, the most noteworthy being presented by Glauert and Lock in references 1 and 2. The validity of the analyses made has not at the present time been established, however, so their application to the problems of design has been impossible. The purpose of this investigation is to extend the analysis of Lock to include the influence of a linear variation of blade pitch with radius and to determine the influence of several factors neglected by him. The resultant analysis is then applied to a comparison of calculated and experimental characteristics, the experimental data being obtained from references 3 and 4.

Lock's analysis is not applicable to a rotor employing twisted blades, so the extension of his treatment will materially increase its usefulness. The majority of rotors now in service have a pitch varying with the radius, as had the PCA-2 rotor which has been tested (references 3 and 4) and used herein to determine the validity of the modified analysis. The comparison of calculated and experimental results will afford a measure of the quantitative validity of the analysis, and assist the designer in obtaining the optimum rotor for a given purpose. The establishment of definite relationships between the rotor design parameters and its characteristics will greatly facilitate research directed toward the improvement of autogiro performance and the analysis of the results of isolated tests.

The investigation presented in this report was conducted by the National Advisory Committee for Aeronautics at Langley Field, Va., during 1933.

ANALYSIS

1. **General.**—The method used in this analysis is in most respects identical with Lock's treatment (reference 2), but the development will in the interests of clarity be repeated. The changes that are to be made in his analysis in an attempt to refine it may be

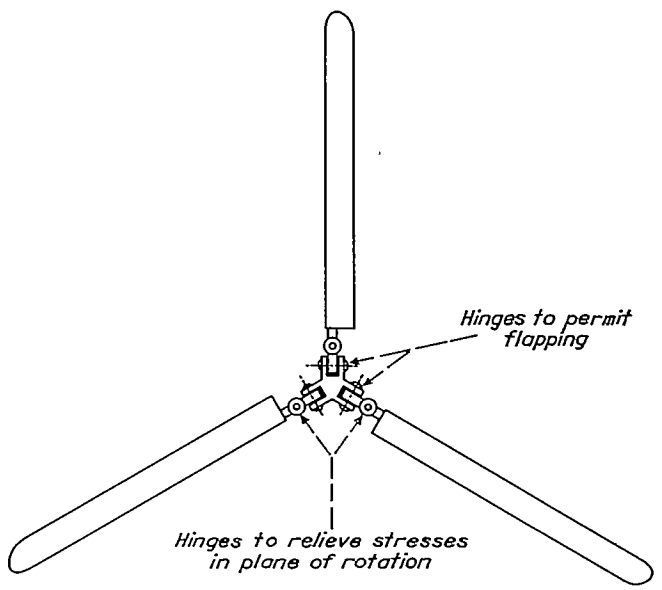

Figure 1.—Diagram of autogiro rotor.

summarized as follows: The limitation of the analysis to blades of constant pitch is removed so that any linear pitch variation may be introduced; an approximate method of evaluating the influence of the reversed flow over the retreating blade is developed; a method of allowing approximately for tip losses in calculating thrust is introduced; and a method of calculating the drag coefficient at 90° angle of attack is given. In respect to the last item, it is subsequently suggested that the calculation of rotor characteristics be done by two separate methods, one for low incidence and one for high incidence.

2. **Mechanics of the rotor.**—The autogiro rotor is a windmill operating at large angles of yaw. In order to eliminate rolling moments in forward flight, the individual blades are hinged near the axis of rotation so as to permit them to oscillate without mechanical constraint in planes containing the axis of rotation.

A diagram of such a rotor is shown in figure 1, where, in addition to the flapping hinges, hinges are shown whose function is the relief of stresses set up by bending in the plane of rotation. Insofar as the aerodynamic effect is concerned, the motion of the blades about these auxiliary hinges may be neglected; experimental values of this motion show the maximum amplitude of the oscillation about the hinge to be less than 1°.

3. Coefficients.—The thrust T of the rotor is expressed as a nondimensional coefficient C_T based on the swept-disk area and the rotational speed of the rotor; then

$$C_T=\frac{T}{\rho\Omega^2\pi R^4} \tag{3–1}$$

where R is the rotor radius
Ω is the rotor angular velocity

The lift and drag coefficients of the rotor are based on the forward speed V rather than the tip speed; then in conventional form,

$$C_{L_r}=\frac{L_r}{\frac{1}{2}\rho V^2\pi R^2} \tag{3–2}$$

and

$$C_{D_r}=\frac{D_r}{\frac{1}{2}\rho V^2\pi R^2} \tag{3–3}$$

where L_r is the rotor lift
D_r is the rotor drag
C_{L_r} is the rotor lift coefficient
C_{D_r} is the rotor drag coefficient

By the use of a nondimensional ratio between the component of forward speed in the plane of the rotor disk and the tip speed, coefficients based on one speed may be expressed in terms of the other. The ratio is called μ, and is expressed as

$$\mu=\frac{V\cos\alpha}{\Omega R} \tag{3–4}$$

where α, the angle of attack of the rotor, is the acute angle between the direction of flow of the undisturbed air and the plane perpendicular to the rotor axis.

The thrust coefficient may be transformed into the lift coefficient by making the assumption, which experience has shown to be valid, that the rotor force perpendicular to the thrust contributes a negligible amount to the lift. Then

$$L_r=T\cos\alpha \tag{3–5}$$

and

$$C_{L_r}=\frac{2C_T\cos^3\alpha}{\mu^2} \tag{3–6}$$

4. Interference flow.—In the vicinity of the rotor, the rotor forces generate local induced velocities which alter the undisturbed flow. The resultant rotor force differs negligibly in direction and magnitude from the thrust, so the component of induced velocity parallel to the rotor axis will be calculated from the thrust, and the remaining components neglected.

The complexity of the flow in the neighborhood of the rotor makes it impossible to solve rigorously for the magnitude and distribution of the induced velocity in the rotor disk. By physical reasoning, however, it may be inferred that the trailing vortices behind the rotor are similar in effect to the vortices behind an airfoil, and it will be assumed that the induced velocity at the rotor disk is constant in magnitude and may be obtained by analogy with airfoil theory. Then a rotor of span $2R$ and total thrust T, distributed elliptically along the span, generates a constant induced velocity expressed by the equation

$$v=\frac{T}{2\pi R^2\rho V'} \tag{4–1}$$

where v is the induced velocity
and V' is the resultant air velocity at the rotor

The influence of an arbitrary deviation from the assumed type of flow will be determined and discussed subsequently.

The resultant velocity at the rotor is the vector sum of the translational and induced velocities. Then

$$V'^2=(V\sin\alpha-v)^2+V^2\cos^2\alpha \tag{4–2}$$

The axial flow is conveniently expressed as $\lambda\Omega R$, and the flow in the plane of the rotor disk as $\mu\Omega R$; then

$$\lambda\Omega R=V\sin\alpha-v \tag{4–3}$$

$$\mu\Omega R=V\cos\alpha \tag{4–4}$$

The resultant velocity can now be written

$$V'=\Omega R(\lambda^2+\mu^2)^{\frac{1}{2}} \tag{4–5}$$

Substituting for T and V' from (3–1) and (4–5), equation (4–1) becomes

$$v=\frac{\frac{1}{2}C_T\Omega R}{(\lambda^2+\mu^2)^{\frac{1}{2}}} \tag{4–6}$$

5. Angle of attack.—Equation (4–3) can be altered to express the angle of attack α as a function of the remaining variables. Substituting for v from (4–6),

$$\lambda\Omega R=V\sin\alpha-\frac{\frac{1}{2}C_T\Omega R}{(\lambda^2+\mu^2)^{\frac{1}{2}}} \tag{5–1}$$

Dividing by (4–4) and transposing,

$$\tan\alpha=\frac{\lambda}{\mu}+\frac{\frac{1}{2}C_T}{\mu(\lambda^2+\mu^2)^{\frac{1}{2}}} \tag{5–2}$$

6. Blade motion.—The flapping motion of the blades is repeated identically with each revolution and is therefore expressed as a Fourier series in which the independent variable is ψ, the azimuth angle of the blade from its downwind position. The Fourier series expresses the acute angle β between the blade span axis and the plane perpendicular to the rotor axis (the rotor disk) as a function of ψ, the form being

$$\beta=a_o-a_1\cos\psi-b_1\sin\psi-a_2\cos 2\psi -b_2\sin 2\psi-a_3\cos 3\psi-b_2\sin 3\psi-\ldots\ldots \tag{6–1}$$

All harmonics above the second have been found experimentally to be negligible, so for use in this analysis the series will be terminated after the b_2 term.

The dynamic equation of blade flapping is

$$I_1\frac{d^2\beta}{dt^2}=\int_o^{BR} r\frac{dT_1}{dr}\cos\beta\,dr - \int_o^R m\Omega^2 r^2\cos\beta\sin\beta\,dr - \int_o^R gmr\cos\beta\,dr \qquad (6\text{–}2)$$

where I_1 is the moment of inertia of one blade about the flapping hinge

$\frac{dT_1}{dr}$ is the thrust on an element dr of one blade

m is the line density of a blade

BR is the radius less an allowance for tip losses

In the application of equation (6–2) it will be assumed that β is small, so that $\cos\beta$ is unity, and $\sin\beta$ is identical with β. Experience has indicated that β has a maximum value of less than 15°, so the assumption is considered justified.

Referring to (6–2), it will be noted that $\int_o^R mr^2\,dr=I_1$; then (6–2) reduces to

$$I_1\left(\frac{d^2\beta}{dt^2}+\Omega^2\beta\right)=M_T-M_W \qquad (6\text{–}3)$$

where M_T is the thrust moment of one blade about the flapping hinge

M_W is the moment of the blade weight about the flapping hinge

7. Velocity components at blade element.—The three orthogonal velocity components at the blade element dr are designated U_T, U_R, and U_P. The component U_T is parallel to the rotor disk and perpendicular to the blade span axis; U_R is parallel to the blade span axis and perpendicular to U_T; and U_P is perpendicular to the span axis and to U_T. Referring to figure 2, the following expressions may be written for the velocities:

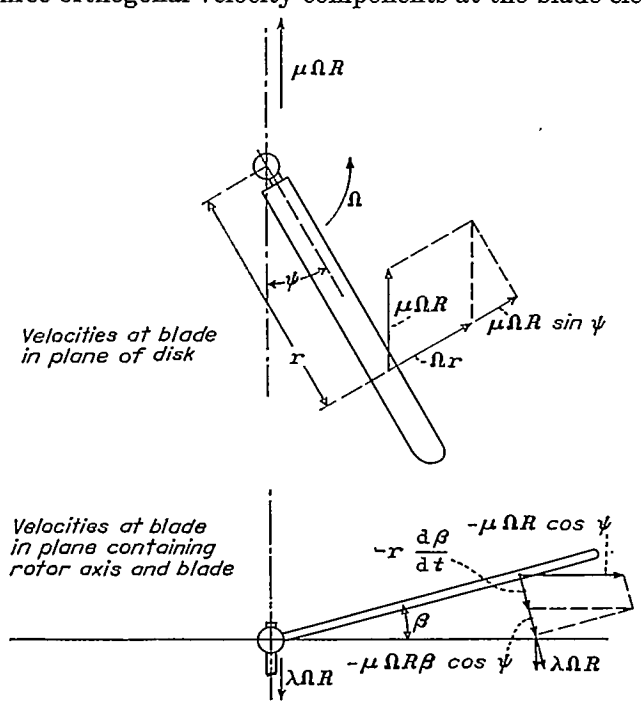

FIGURE 2.—Velocity components at blade element of autogiro rotor blade.

$$U_T=\Omega r+\mu\Omega R\sin\psi \qquad (7\text{–}1)$$

$$U_P=\lambda\Omega R-r\frac{d\beta}{dt}-\mu\Omega R\beta\cos\psi \qquad (7\text{–}2)$$

$$U_R=\mu\Omega R\cos\psi+\lambda\Omega R\beta \qquad (7\text{–}3)$$

Differentiating the expression for β in (6–1), and substituting for β and $\frac{d\beta}{dt}$ in (7–2),

$$U_P=\lambda\Omega R+\frac{1}{2}\mu\Omega Ra_1+\left(-\mu\Omega Ra_0+\Omega rb_1+\frac{1}{2}\mu\Omega Ra_2\right)\cos\psi +\left(-\Omega ra_1+\frac{1}{2}\mu\Omega Rb_2\right)\sin\psi +\left(\frac{1}{2}\mu\Omega Ra_1+2\Omega rb_2\right)\cos 2\psi+\left(\frac{1}{2}\mu\Omega Rb_1-2\Omega ra_2\right)\sin 2\psi +\frac{1}{2}\mu\Omega Ra_2\cos 3\psi+\frac{1}{2}\mu\Omega Rb_2\sin 3\psi \qquad (7\text{–}4)$$

8. Thrust.—In the calculation of the forces acting on the blade element it will be assumed that the resultant force lies in a plane perpendicular to the blade span axis and depends only upon the velocities in that plane. This assumption is equivalent to neglecting the influence of the radial velocity U_R on the blade forces. It will be further assumed that the drag of the blade element contributes a negligible amount to the rotor thrust.

The resultant velocity U of U_T and U_P makes an acute angle φ with the velocity U_T; then

$$U_T=U\cos\varphi \qquad (8\text{–}1)$$

$$U_P=U\sin\varphi \qquad (8\text{–}2)$$

Over the greater part of the rotor blades, and especially where U is large, the angle φ is small. For this reason, it will be assumed that the sine of φ is equal to φ and that the cosine of φ is unity. Equations (8–1) and (8–2) then reduce to

$$U_T=U \qquad (8\text{–}3)$$

$$U_P=\varphi U \qquad (8\text{–}4)$$

In order to set up the integral for the evaluation of the thrust it must be remembered that the blade velocity is reversed over the elements from a radius of 0 to $-\mu R\sin\psi$. This condition does not indicate a negative contribution to the thrust, but requires a special integral for its evaluation. In the derivation of the total thrust, an approximate allowance will be made for tip losses by integrating to a fraction of the radius. It is arbitrarily suggested that this fraction be chosen so that a tip length equal to one-half the tip chord is assumed to develop no thrust.

The lift coefficient C_L of the blade element is assumed to be proportional to the angle of attack, an assumption that is valid for lift coefficients less than the maximum. Then

$$C_L=a\alpha_r \qquad (8\text{–}5)$$

where a is the lift-curve slope with angle of attack, in radian measure

α_r is the blade-element angle of attack in radians, measured from zero lift

The blade-element angle of attack is the sum of the pitch angle θ (also measured from zero lift) and the angle φ of the resultant velocity to the rotor disk. (See fig. 3.) Assuming that θ varies linearly with the radius

$$\theta=\theta_0+\frac{r}{R}\theta_1 \tag{8-6}$$

Then

$$\alpha_r=\theta_0+\frac{r}{R}\theta_1+\varphi \tag{8-7}$$

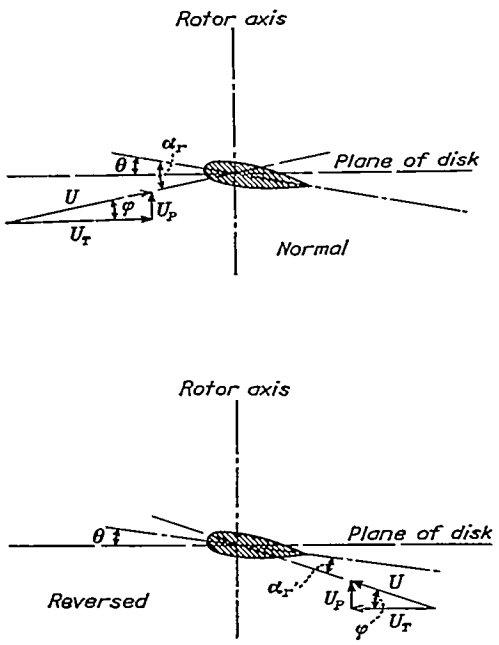

FIGURE 3.—Angle of attack diagram of blade element of autogiro rotor.

The preceding expression for α_r is true only when the direction of the resultant velocity is such that the flow is from the leading to the trailing edge of the element. When this direction of flow is reversed, consideration of the definition of φ becomes necessary in order to express the angle of attack.

It is seen from equations (8–3) and (8–4) that

$$\varphi=\frac{U_P}{U_T} \tag{8-8}$$

When U_T changes sign and U_P does not, φ also changes sign; furthermore, φ is the acute angle between the velocity U and the rotor disk. A positive angle of attack is defined as one that results in a positive thrust; a negative φ in the reversed-velocity region then contributes a positive component to the angle of attack, and a positive pitch angle contributes a negative component to the angle of attack. The angle of attack α_r' in the reversed-velocity region can then be written from figure 3,

$$\alpha_r'=-\theta_0-\frac{r}{R}\theta_1-\varphi \tag{8-9}$$

The thrust will be evaluated on the basis of the assumption, previously stated, that β and φ are small. Then if b is the number of blades and c the blade chord, assumed constant, the thrust T becomes

$$T=\frac{b}{2\pi}\int_0^{2\pi}\mathrm{d}\psi\int_0^{BR}\frac{1}{2}\rho cU^2C_L\mathrm{d}r \tag{8-10}$$

The evaluation of the integral for the thrust is possible only when the expression is split up and the influence of the reversed velocity taken into account. It will be assumed for simplicity that the lift-curve slope at 180° angle of attack is equal to that at 0°; then

$$\begin{aligned}T=&\frac{b}{2\pi}\int_0^{\pi}\mathrm{d}\psi\int_0^{BR}\frac{1}{2}\rho caU^2\left(\theta_0+\frac{r}{R}\theta_1+\varphi\right)\mathrm{d}r\\&+\frac{b}{2\pi}\int_{\pi}^{2\pi}\mathrm{d}\psi\int_{-\mu R\sin\psi}^{BR}\frac{1}{2}\rho caU^2\left(\theta_0+\frac{r}{R}\theta_1+\varphi\right)\mathrm{d}r\\&+\frac{b}{2\pi}\int_{\pi}^{2\pi}\mathrm{d}\psi\int_0^{-\mu R\sin\psi}\frac{1}{2}\rho caU^2\left(-\theta_0-\frac{r}{R}\theta_1-\varphi\right)\mathrm{d}r\end{aligned} \tag{8-11}$$

The integration of (8–11) is performed after rearranging and substituting for U^2 and φU^2 the identities obtained from (8–3) and (8–4)—that is, $U^2=U_T^2$ and $\varphi U^2=U_T\,U_P$. Then

$$\begin{aligned}T=&\frac{b}{2\pi}\int_0^{2\pi}\mathrm{d}\psi\int_0^{BR}\frac{1}{2}\rho ca\left\{\left(\theta_0+\frac{r}{R}\theta_1\right)U_T^2+U_TU_P\right\}\mathrm{d}r\\&-\frac{b}{\pi}\int_0^{2\pi}\mathrm{d}\psi\int_0^{-\mu R\sin\psi}\frac{1}{2}\rho ca\left\{\left(\theta_0+\frac{r}{R}\theta_1\right)U_T^2+U_TU_P\right\}\mathrm{d}r\\=&\frac{1}{2}bc\rho a\,\Omega^2R^3\left\{\frac{1}{2}\lambda\left(B^2+\frac{1}{2}\mu^2\right)+\theta_0\left(\frac{1}{3}B^3+\frac{1}{2}\mu^2B-\frac{4}{9\pi}\mu^3\right)\right.\\&\left.+\theta_1\left(\frac{1}{4}B^4+\frac{1}{4}\mu^2B^2-\frac{1}{32}\mu^4\right)+\frac{1}{4}\mu^2b_2B+\frac{1}{8}\mu^3a_1\right\}\end{aligned} \tag{8-12}$$

where terms of higher order in μ than the fourth are neglected. The ratio between the total blade area and the swept-disk area of the rotor is termed the solidity, and for rectangular blades is

$$\sigma=\frac{bc}{\pi R} \tag{8-13}$$

from equations (3–1), (8–12), and (8–13), the thrust coefficient of the rotor is

$$\begin{aligned}C_T=&\frac{1}{2}\sigma a\left\{\frac{1}{2}\lambda\left(B^2+\frac{1}{2}\mu^2\right)\right.\\&+\theta_0\left(\frac{1}{3}B^3+\frac{1}{2}\mu^2B-\frac{4}{9\pi}\mu^3\right)\\&+\theta_1\left(\frac{1}{4}B^4+\frac{1}{4}\mu^2B^2-\frac{1}{32}\mu^4\right)\\&\left.+\frac{1}{4}\mu^2b_2B+\frac{1}{8}\mu^3a_1\right\}\end{aligned} \tag{8-14}$$

9. Thrust moment.—The moment of the thrust M_T about the flapping hinge is, neglecting the radial distance from the axis of rotation to the axis of the hinge,

$$M_T=\int_0^{BR}\frac{1}{2}\rho cU^2C_Lr\mathrm{d}r \tag{9-1}$$

Substituting as in (8–10), and taking into account the influence of the reversed velocities,

$$M_T=\int_0^{BR}\frac{1}{2}\rho ca\left\{\left(\theta_0+\frac{r}{R}\theta_1\right)U_T^2+U_TU_P\right\}r\mathrm{d}r$$
$$-2\int_0^{-\mu R\sin\psi}\frac{1}{2}\rho ca\left\{\left(\theta_0+\frac{r}{R}\theta_1\right)U_T^2+U_TU_P\right\}r\mathrm{d}_P\Bigg]_\pi^{2\pi} \quad (9\text{–}2)$$

Where $\Big]_\pi^{2\pi}$ indicates that the second expression enters into the thrust moment only in the interval between $\psi=\pi$ and $\psi=2\pi$.

In order to obtain a single expression for the thrust moment at any value of ψ, the problem of combining a general expression extending from 0 to 2π with another extending from π to 2π was analyzed. A Fourier series of the type

$$Y=a_0+a_1\cos\psi+b_1\sin\psi+a_2\cos 2\psi+b_2\sin 2\psi \quad (9\text{–}3)$$

extending from 0 to 2π, has added to it the series

$$\Delta Y=\Delta a_0+\Delta a_1\cos\psi+\Delta b_1\sin\psi+\Delta a_2\cos 2\psi+\Delta b_2\sin 2\psi \quad (9\text{–}4)$$

which extends from π to 2π. By harmonic analysis the resultant series, continuous at π and 2π,

$$Y_R=A_0+A_1\cos\psi+B_1\sin\psi+A_2\cos 2\psi+B_2\sin 2\psi \quad (9\text{–}5)$$

was obtained, and the following relations established:

$$\left.\begin{aligned}
\Delta a_0&=-\Delta a_2\\
\Delta a_1&=0\\
A_0&=a_0+0.500\Delta a_0-0.318\Delta b_1\\
A_1&=a_1-0.424\Delta b_2\\
B_1&=b_1-0.849\Delta a_0+0.500\Delta b_1\\
A_2&=a_2-0.500\Delta a_0-0.212\Delta b_1\\
B_2&=b_2+0.500\Delta b_2
\end{aligned}\right\} \quad (9\text{–}6)$$

The relations expressed in the first two equations follow from the condition of continuity.

Integrating (9–2), combining the two integrals into one expression by (9–6), and dropping all terms of order greater than μ^4,

$$\frac{M_T}{\frac{1}{2}\rho ca\Omega^2R^4}=\frac{1}{3}\lambda B^3+0.080\mu^3\lambda$$
$$+\frac{1}{4}\theta_0\left(B^4+\mu^2B^2-\frac{1}{8}\mu^4\right)$$
$$+\frac{1}{5}\theta_1\left(B^5+\frac{5}{6}\mu^2B^3\right)+\frac{1}{8}\mu^2b_2B^2$$
$$+\left\{\frac{2}{3}\mu\theta_0B^3+0.053\mu^4\theta_0+\frac{1}{2}\mu\theta_1B^4-\frac{1}{4}a_1B^4\right.$$
$$\left.-\frac{1}{6}\mu b_2B^3+\frac{1}{2}\mu\lambda B^2-\frac{1}{8}\mu^3\lambda+\frac{1}{8}\mu^2a_1B^2\right\}\sin\psi$$
$$+\left\{-\frac{1}{3}\mu a_0B^3-0.035\mu^4a_0+\frac{1}{4}b_1B^4-\frac{1}{6}\mu a_2B^3\right.$$
$$\left.+\frac{1}{8}\mu^2b_1B^2\right\}\cos\psi$$
$$+\left\{\frac{1}{3}\mu b_1B^3-\frac{1}{2}a_2B^4-\frac{1}{4}\mu^2a_0B^2+\frac{1}{24}\mu^4a_0\right\}\sin 2\psi$$
$$+\left\{-\frac{1}{4}\mu^2\theta_0B^2+\frac{1}{32}\mu^4\theta_0-\frac{1}{6}\mu^2\theta_1B^3+\frac{1}{2}b_2B^4\right.$$
$$\left.+\frac{1}{3}\mu a_1B^3-0.053\mu^3\lambda\right\}\cos 2\psi \quad (9\text{–}7)$$

From (6–3), substituting for β and $\frac{\mathrm{d}^2\beta}{\mathrm{d}t^2}$ from (6–1),

$$I_1\Omega^2(a_0+3a_2\cos 2\psi+3b_2\sin 2\psi)=M_T-M_W \quad (9\text{–}8)$$

After substituting for M_T from (9–7), the following set of equations is obtained by equating coefficients of identical trigonometric functions:

$$\left.\begin{aligned}
a_0&=\frac{\frac{1}{2}\rho caR^4}{I_1}\left\{\frac{1}{3}\lambda B^3+0.080\mu^3\lambda+\frac{1}{4}\theta_0\left(B^4+\mu^2B^2-\frac{1}{8}\mu^4\right)\right.\\
&\quad\left.+\frac{1}{5}\theta_1\left(B^5+\frac{5}{6}\mu^2B^3\right)+\frac{1}{8}\mu^2b_2B^2\right\}-\frac{M_W}{I_1\Omega^2}\\
0&=-\frac{1}{3}\mu a_0B^3+\frac{1}{4}b_1B^4-\frac{1}{6}\mu a_2B^3+\frac{1}{8}\mu^2b_1B^2\\
&\quad-0.035\mu^4a_0\\
0&=\frac{2}{3}\mu\theta_0B^3+0.053\mu^4\theta_0+\frac{1}{2}\mu\theta_1B^4-\frac{1}{4}a_1B^4\\
&\quad-\frac{1}{6}\mu b_2B^3+\frac{1}{2}\mu\lambda B^2-\frac{1}{8}\mu^3\lambda+\frac{1}{8}\mu^2a_1B^2\\
\frac{3I_1}{\frac{1}{2}\rho caR^4}a_2&=-\frac{1}{4}\mu^2\theta_0B^2+\frac{1}{32}\mu^4\theta_0-\frac{1}{6}\mu^2\theta_1B^3\\
&\quad+\frac{1}{2}b_2B^4+\frac{1}{3}\mu a_1B^3-0.053\mu^3\lambda\\
\frac{3I_1}{\frac{1}{2}\rho caR^4}b_2&=\frac{1}{3}\mu b_1B^3-\frac{1}{2}a_2B^4-\frac{1}{4}\mu^2a_0B^2+\frac{1}{24}\mu^4a_0
\end{aligned}\right\} \quad (9\text{–}9)$$

Let

$$\gamma=\frac{c\rho aR^4}{I_1} \quad (9\text{–}10)$$

where γ is a nondimensional coefficient that represents the mass constant of the blade and expresses the relationship between the air forces and mass forces acting on the blade. Using (9–10) in (9–9), and simplifying,

$$\left.\begin{aligned}
a_0 &= \frac{1}{2}\gamma\left\{\frac{1}{3}\lambda B^3+0.080\mu^3\lambda+\frac{1}{4}\theta_0\left(B^4+\mu^2B^2-\frac{1}{8}\mu^4\right)\right.\\
&\qquad\left.+\frac{1}{5}\theta_1\left(B^5+\frac{5}{6}\mu^2B^3\right)+\frac{1}{8}\mu^2b_2B^2\right\}-\frac{M_W}{I_1\Omega^2}\\
a_1 &= \frac{2\mu}{B^4-\frac{1}{2}\mu^2B^2}\left\{\lambda\left(B^2-\frac{1}{4}\mu^2\right)+\frac{4}{3}\theta_0B^3+0.106\mu^3\theta_0\right.\\
&\qquad\left.+\theta_1B^4-\frac{1}{3}b_2B^3\right\}\\
b_1 &= \frac{4\mu B}{B^2+\frac{1}{2}\mu^2}\left\{\frac{1}{3}a_0+\frac{0.035}{B^3}\mu^3a_0+\frac{1}{6}a_2\right\}\\
3a_2-\frac{1}{4}\gamma b_2B^4 &= \frac{1}{2}\gamma\mu^2\left\{-\frac{1}{4}\theta_0\left(B^2-\frac{1}{8}\mu^2\right)\right.\\
&\qquad\left.-\frac{1}{6}\theta_1B^3-0.053\mu\lambda+\frac{1}{3}\frac{a_1}{\mu}B^3\right\}\\
3b_2+\frac{1}{4}\gamma a_2B^4 &= \frac{1}{2}\gamma\mu^2\left\{-\frac{1}{4}a_0\left(B^2-\frac{1}{6}\mu_2\right)\right.\\
&\qquad\left.+\frac{1}{3}\frac{b_1}{\mu}B^3\right\}
\end{aligned}\right\}\quad(9\text{–}11)$$

Inspection of (9–11) shows that a_0 is of the order of μ^0, a_1 and b_1 are of the order of μ, and a_2 and b_2 are of the order of μ^2. It will be shown in section 10 that in order to evaluate the torque equation including all terms whose order is μ^4 or lower, the expressions for a_0, a_2, and b_2 must be carried out to the order of μ^2, and the expressions for a_1 and b_1 to the order of μ^3. To this approximation, the expressions for a_2 and b_2 in (9–11) become

$$\left.\begin{aligned}
3a_2-\frac{1}{4}\gamma b_2B^4 &= \frac{1}{2}\gamma\mu^2\left\{-\frac{1}{4}\theta_0B^2-\frac{1}{6}\theta_1B^3+\frac{1}{3}\frac{a_1}{\mu}B^3\right\}\\
3b_2+\frac{1}{4}\gamma a_2B^4 &= \frac{1}{2}\gamma\mu^2\left\{-\frac{1}{4}a_0B^2+\frac{1}{3}\frac{b_1}{\mu}B^3\right\}
\end{aligned}\right\}\quad(9\text{–}12)$$

The following approximations are sufficiently accurate for substitution in (9–12):

$$\left.\begin{aligned}
a_0 &= \frac{1}{2}\gamma\left\{\frac{1}{3}\lambda B^3+\frac{1}{4}\theta_0B^4+\frac{1}{5}\theta_1B^5\right\}\\
a_1 &= \frac{2\mu}{B^4}\left\{\lambda B^2+\frac{4}{3}\theta_0B^3+\theta_1B^4\right\}\\
b_1 &= \frac{4\mu}{3B}a_0
\end{aligned}\right\}\quad(9\text{–}13)$$

Substituting in (9–12) from (9–13),

$$\left.\begin{aligned}
3a_2-\frac{1}{4}\gamma b_2B^4 &= \frac{1}{2}\gamma\mu^2\left\{\frac{2}{3}\lambda B+\frac{23}{36}\theta_0B^2+\frac{1}{2}\theta_1B^3\right\}\\
\frac{1}{4}\gamma a_2B^4+3b_2 &= \frac{1}{2}\gamma^2\mu^2\left\{\frac{7}{216}\lambda B^5+\frac{7}{288}\theta_0B^6+\frac{7}{360}\theta_1B^7\right\}
\end{aligned}\right\}\quad(9\text{–}14)$$

Solving (9–14) for a_2 and b_2,

$$\left.\begin{aligned}
a_2 &= \frac{\gamma\mu^2}{144+\gamma^2B^8}\left\{\lambda B\left(16+\frac{7}{108}\gamma^2B^8\right)+\theta_0B^2\left(\frac{46}{3}\right.\right.\\
&\qquad\left.\left.+\frac{7}{144}\gamma^2B^8\right)+\theta_1B^3\left(12+\frac{7}{180}\gamma^2B^8\right)\right\}\\
b_2 &= \frac{-\gamma^2\mu^2}{144+\gamma^2B^8}\left\{\frac{5}{9}\lambda B^5+\frac{25}{36}\theta_0B^6+\frac{8}{15}\theta_1B^7\right\}
\end{aligned}\right\}\quad(9\text{–}15)$$

The expressions for a_2 and b_2 in (9–15) may be substituted in (9–11) for a_2 and b_2 where they occur in the expressions for a_0, a_1, and b_1; the flapping is then completely expressed by coefficients that are given in terms of μ, λ, and the physical constants of the blade.

10. Torque.—The aerodynamic torque on an element of the blade is made up of the components in the rotor disk of the lift and drag of the element. As previously stated, in resolving the lift and drag into their components the sine of φ will be assumed equal to φ and cos φ equal to unity. It will also be assumed that a single average value may be assigned to the drag coefficient of any element, the suggested value being one and one-half times the minimum drag coefficient of the airfoil section. Since large angles of attack and large drag coefficients are attained only in regions of low velocity, where the contribution to the net torque is small, the average value chosen is felt to be conservative.

In a steady state of rotation the torque is zero. Then

$$\begin{aligned}
Q=0 &= \frac{b}{2\pi}\int_0^{2\pi}d\psi\int_0^{BR}\frac{1}{2}\rho cU^2\varphi C_Lr\,dr\\
&\quad-\frac{b}{2\pi}\int_0^{2\pi}d\psi\int_0^{R}\frac{1}{2}\rho cU^2\delta r\,dr
\end{aligned}\qquad(10\text{–}1)$$

where δ is the average drag coefficient.

Taking limits so that the region of reversed velocities is properly expressed, (10–1) becomes upon substituting from (8–5), (8–7), and (8–9)

$$\begin{aligned}
0 &= \frac{b}{2\pi}\int_0^{\pi}d\psi\int_0^{BR}\frac{1}{2}\rho ca\left(\varphi\theta_0+\frac{r}{R}\varphi\theta_1+\varphi^2\right)U^2r\,dr\\
&\quad+\frac{b}{2\pi}\int_{\pi}^{2\pi}d\psi\int_{-\mu R\sin\psi}^{BR}\frac{1}{2}\rho ca\left(\varphi\theta_0+\frac{r}{R}\varphi\theta_1+\varphi^2\right)U^2r\,dr\\
&\quad-\frac{b}{2\pi}\int_{\pi}^{2\pi}d\psi\int_0^{-\mu R\sin\psi}\frac{1}{2}\rho ca\left(\varphi\theta_0+\frac{r}{R}\varphi\theta_1+\varphi^2\right)U^2r\,dr\\
&\quad-\frac{b}{2\pi}\int_0^{\pi}d\psi\int_0^{R}\frac{1}{2}\rho c\delta U^2r\,dr\\
&\quad-\frac{b}{2\pi}\int_{\pi}^{2\pi}d\psi\int_{-\mu R\sin\psi}^{R}\frac{1}{2}\rho c\delta U^2r\,dr\\
&\quad+\frac{b}{2\pi}\int_{\pi}^{2\pi}d\psi\int_0^{-\mu R\sin\psi}\frac{1}{2}\rho c\delta U^2r\,dr
\end{aligned}\qquad(10\text{–}2)$$

Rearranging and substituting from (8–3) and (8–4),

$$0=\int_0^{2\pi}\mathrm{d}\psi\int_0^{BR}a\left\{U_TU_P\left(\theta_0+\frac{r}{R}\theta_1\right)+U_P^2\right\}r\mathrm{d}r$$
$$-2\int_\pi^{2\pi}\mathrm{d}\psi\int_0^{-\mu R\sin\psi}a\left\{U_TU_P\left(\theta_0+\frac{r}{R}\theta_1\right)+U_P^2\right\}r\mathrm{d}r$$
$$-\int_0^{2\pi}\mathrm{d}\psi\int_0^{R}\delta U_T^2r\mathrm{d}r$$
$$+2\int_\pi^{2\pi}\mathrm{d}\psi\int_0^{-\mu R\sin\psi}\delta U_T^2r\mathrm{d}r \qquad (10\text{–}3)$$

Substitute from (7–1) and (7–4) for U_T and U_P; integrate and simplify; then, neglecting terms of higher order than μ^4,

$$\lambda^2\left(\frac{1}{2}B^2-\frac{1}{4}\mu^2\right)+\lambda\left(\frac{1}{3}\theta_0B^3+\frac{2}{9\pi}\mu^3\theta_0+\frac{1}{4}\theta_1B^4+\frac{1}{32}\mu^4\theta_1\right)$$
$$+\mu\lambda a_1\left(\frac{1}{2}B^2-\frac{3}{8}\mu^2\right)+a_0^2\left(\frac{1}{4}\mu^2B^2-\frac{1}{16}\mu^4\right)$$
$$-\frac{1}{3}\mu a_0b_1B^3+a_1^2\left(\frac{1}{8}B^4+\frac{3}{16}\mu^2B^2\right)$$
$$+b_1^2\left(\frac{1}{8}B^4+\frac{1}{16}\mu^2B^2\right)-a_2\left(\frac{1}{4}\mu^2a_0B^2+\frac{1}{6}\mu b_1B^3\right)$$
$$+\frac{1}{2}a_2^2B^4+b_2\left(\frac{1}{8}\mu^2\theta_0B^2+\frac{1}{12}\mu^2\theta_1B^3+\frac{1}{6}\mu a_1B^3\right)$$
$$+\frac{1}{2}b_2^2B^4-\frac{\delta}{4a}\left(1+\mu^2-\frac{1}{8}\mu^4\right)=0 \qquad (10\text{–}4)$$

It should be noted that the drag term in (10–1) is integrated to the tip, while the thrust term is integrated only to BR. This method is considered advisable, inasmuch as tip losses in reducing thrust certainly do not decrease the profile drag.

Examination of (10–4) verifies the statement previously made that, in order to include all terms of order μ^4 or lower in the torque equation, it is necessary to evaluate a_0, a_2, and b_2 to the order μ^2 and a_1 and b_1 to the order μ^3. It has been shown in (9–11) and (9–15) that the blade-motion coefficients a_0, a_1, b_1, a_2, and b_2 are linear functions of λ; the torque equation is then a quadratic in λ and its solution for a series of values of μ is simple. By the use of the torque equation λ can be obtained as a function of μ; the physical interpretation of the solution is that of finding for a rotor of given geometric form, the magnitude of the axial flow through the rotor disk which results in a state of steady autorotation.

11. Lift-drag ratio.—The simplest and most direct method of evaluating the drag of the rotor is that of considering the energy lost in the rotor. There are two channels through which energy is dissipated: in the generation of thrust, and in the losses arising from the blade drag. Placing the total energy loss per second equal to D_rV where D_r is the rotor drag,

$$D_rV=vT+\frac{b}{2\pi}\int_0^{2\pi}\mathrm{d}\psi\int_0\ \frac{1}{2}\rho c\delta U_T^3\mathrm{d}r$$
$$-\frac{b}{\pi}\int_\pi^{2\pi}\mathrm{d}\psi\int_0^{-\mu R\sin\psi}\frac{1}{2}\rho c\delta U_T^3\mathrm{d}r \qquad (11\text{–}1)$$

The drag integral in (11–1) has been set up in accordance with similar previous expressions to allow for the influence of the reversed velocities, since regardless of the direction of the velocity there is an energy loss, and the first integral expresses that loss incorrectly in the reversed-velocity region. Upon integrating, (11–1) becomes

$$D_rV=\frac{1}{2}bc\rho\Omega^3R^4\delta\left(\frac{1}{4}+\frac{3}{4}\mu^2+\frac{3}{32}\mu^4\right)+vT \qquad (11\text{–}2)$$

From equation (3–5), $L_r=T\cos\alpha$; dividing (11–2) by $L_rV=T\,V\cos\alpha$,

$$\frac{D_r}{L_r}=\delta\left(\frac{1}{4}+\frac{3}{4}\mu^2+\frac{3}{32}\mu^4\right)\frac{\frac{1}{2}bc\rho\Omega^3R^4}{TV\cos\alpha}+\frac{v}{V\cos\alpha} \qquad (11\text{–}3)$$

Substitute for v from (4–6), for V from (3–4), and for T from (3–1); then

$$\frac{D_r}{L_r}=\frac{\sigma\delta\left(1+3\mu^2+\frac{3}{8}\mu^4\right)}{8\mu C_T}+\frac{\frac{1}{2}C_T}{\mu(\mu^2+\lambda^2)^{\frac{1}{2}}} \qquad (11\text{–}4)$$

12. Rotor pitching and rolling moments.—The development of expressions for the aerodynamic characteristics of the rotor has so far assumed that the blades flap about a point on the rotor axis. For most full-scale rotors this assumption is in error, although the distance from axis to hinge is in general so small that the offset may be neglected in considering the motion of the blades. The distance from hinge to axis has, however, an appreciable influence upon the position of the resultant rotor force, which will be evaluated in this section. Let the distance from hinge to axis be designated r_H. The instantaneous thrust T_1 on one blade is, from (8–11)

$$T_1=\int_0^{BR}\frac{1}{2}\rho ca\left(\theta_0+\frac{r}{R}\theta_1\right)U_T^2\mathrm{d}r$$
$$+\int_0^{BR}\frac{1}{2}\rho caU_TU_P\mathrm{d}r \qquad (12\text{–}1)$$

where the corrections for reversed flow are omitted, being considered negligible. The longitudinal center of pressure of the total thrust is obtained by adding together the terms $-T_1r_H\cos\psi$ at positions corresponding to the instantaneous positions of the blades; for four blades, assign ψ successive values differing by $\frac{\pi}{2}$; for three blades, values differing by $\frac{2}{3}\pi$.

Upon integration, (12–1) becomes

$$T_1=\frac{1}{2}\rho ca\Omega^2R^3\left\{\frac{1}{3}\theta_0B^3+\frac{1}{2}\mu^2\theta_0B+\frac{1}{4}\theta_1B^4+\frac{1}{4}\mu^2\theta_1B^2\right.$$
$$+\frac{1}{2}\lambda B^2+\frac{1}{4}\mu^2b_2B$$
$$+\left(-\frac{1}{2}\mu a_0B^2+\frac{1}{3}b_1\left[B^3+\frac{3}{4}\mu^2B\right]-\frac{1}{4}\mu a_2B^2\right)\cos\psi$$
$$+\left(\mu\theta_0B^2+\frac{2}{3}\mu\theta_1B^3-\frac{1}{3}a_1\left[B^3-\frac{3}{4}\mu^2B\right]+\mu\lambda B\right.$$

$$-\frac{1}{4}\mu b_2B^2\Big)\sin\psi$$
$$+\Big(-\frac{1}{2}\mu^2\theta_0B-\frac{1}{4}\mu^2\theta_1B^2+\frac{1}{2}\mu a_1B^2+\frac{2}{3}b_2B^3\Big)\cos 2\psi$$
$$+\Big(-\frac{1}{2}\mu^2a_0B+\frac{1}{2}\mu b_1B^2-\frac{2}{3}a_2B^3\Big)\sin 2\psi$$
$$+\Big(-\frac{1}{4}\mu^2b_1B+\frac{3}{4}\mu a_2B^2\Big)\cos 3\psi$$
$$+\Big(\frac{1}{4}\mu^2a_1B+\frac{3}{4}\mu b_2B^2\Big)\sin 3\psi$$
$$-\frac{1}{4}\mu^2b_2B\cos 4\psi+\frac{1}{4}\mu^2a_2B\sin 4\psi \qquad (12\text{–}2)$$

By the assignment to ψ in $-T_1r_H\cos\psi$ of four values differing by $\frac{\pi}{2}$ and summing, the pitching moment for a 4-bladed rotor is expressed as

$$M_{t_4}=\frac{1}{2}bc\rho a\Omega^2R^3r_H\Big\{-\frac{1}{4}\mu a_oB^2+\frac{1}{6}b_1\Big(B^3+\frac{3}{4}\mu^2B\Big)$$
$$-\frac{1}{8}\mu a_2B^2+\Big(-\frac{1}{8}\mu^2b_1B+\frac{3}{8}\mu a_2B^2\Big)\cos 4\psi$$
$$+\frac{1}{8}\mu^2a_1B+\frac{3}{8}\mu b_2B^2\Big)\sin 4\psi\Big\} \qquad (12\text{–}3)$$

where M_{t_4} is the rotor pitching moment for four blades. In a similar operation, by assigning to ψ three values differing by $\frac{2}{3}\pi$, the pitching moment is expressed as

$$M_{t_3}=\frac{1}{2}bc\rho a\Omega^2R^3r_H\Big\{-\frac{1}{4}\mu a_oB^2+\frac{1}{6}b_1\Big(B^3+\frac{3}{4}\mu^2B\Big)$$
$$-\frac{1}{8}\mu a_2B^2+\Big(-\frac{1}{4}\mu^2\theta_0B-\frac{1}{8}\mu^2\theta_1B^2+\frac{1}{4}\mu a_1B^2$$
$$+\frac{1}{3}b_2B^3-\frac{1}{8}\mu^2b_2B\Big)\cos 3\psi$$
$$+\Big(-\frac{1}{4}\mu^2a_0B+\frac{1}{4}\mu b_1B^2-\frac{1}{3}a_2B^3$$
$$+\frac{1}{8}\mu^2a_2B\Big)\sin 3\psi\Big\} \qquad (12\text{–}4)$$

where M_{t_3} is the rotor pitching moment for three blades.

The rolling moment is obtained by summing $T_1\ r_H\sin\psi$ at correct intervals of ψ. Then for four blades

$$L_{t_4}=\frac{1}{2}bc\rho a\Omega^2R^3r_H\Big\{\frac{1}{2}\mu\theta_0B^2+\frac{1}{3}\mu\theta_1B^3+\frac{1}{2}\mu\lambda B$$
$$-\frac{1}{6}a_1\Big(B^3-\frac{3}{4}\mu^2B\Big)-\frac{1}{8}\mu b_2B^2$$
$$+\Big(-\frac{1}{8}\mu^2b_1B+\frac{3}{8}\mu a_2B^2\Big)\sin 4\psi$$
$$-\Big(\frac{1}{8}\mu^2a_1B+\frac{3}{8}\mu b_2B^2\Big)\cos 4\psi\Big\} \qquad (12\text{–}5)$$

where L_{t_4} is the rotor rolling moment for four blades.

And

$$L_{t_3}=\frac{1}{2}bc\rho a\Omega^2R^3r_H\Big\{\frac{1}{2}\mu\theta_0B^2+\frac{1}{3}\mu\theta_1B^3+\frac{1}{2}\mu\lambda B$$
$$-\frac{1}{6}a_1\Big(B^3-\frac{3}{4}\mu^2B\Big)-\frac{1}{8}\mu b_2B^2$$
$$+\Big(-\frac{1}{4}\mu^2\theta_0B-\frac{1}{8}\mu^2\theta_1B^2+\frac{1}{4}\mu a_1B^2+\frac{1}{3}b_2B^3$$
$$+\frac{1}{8}\mu^2b_2B\Big)\sin 3\psi$$
$$-\Big(-\frac{1}{4}\mu^2a_0B+\frac{1}{4}\mu b_1B^2-\frac{1}{3}a_2B^3-\frac{1}{8}\mu^2a_2B\Big)\cos 3\psi\Big\} \qquad (12\text{–}6)$$

where L_{t_3} is the rotor rolling moment for three blades.

13. Effect of a varying induced flow.—The autogiro rotor generates an induced velocity that probably differs materially in magnitude, in parts of the rotor disk, from the constant value assumed for simplicity. Since the flapping acts in such a manner as to equalize the thrust on opposite sides of the plane of symmetry, it appears logical to assume a symmetrical distribution of the induced velocity along the Y axis, and the errors incident to this assumption should be of small magnitude. If the rotor is considered as an airfoil with its maximum chord equal to the span, it is reasonable to expect an increase in the magnitude of the induced velocity in passing from the leading to the trailing edge of the disk. In the analysis of the effect upon the rotor of a flow of this type, the simplest case will be treated—that is, one in which the induced velocity increases linearly with distance downstream from the leading edge, and the average induced velocity over the disk is the same in value as that initially obtained. The assumption will be made that there is superposed upon the induced velocity v an additional velocity v_1, expressed as

$$v_1=Kv\frac{r}{R}\cos\psi \qquad (13\text{–}1)$$

where K is the ratio between v_1 and v when $r=R$ and $\cos\psi=1$.

The factor K probably varies with the tip-speed ratio, inasmuch as the distribution of the induced velocity will approach symmetry as the tip-speed ratio approaches zero, and will approach, from physical reasoning, a maximum asymmetry as the tip-speed ratio approaches a maximum. It is impossible in the scope of this investigation to specify any definite variation of K with μ, although subsequently an empirical relation may be obtained.

The mean value over the disk of the induced velocity is unchanged, since at equal values of r and values of ψ differing by π, v_1 will be equal and opposite in sign.

From (4–6), (13–1) may be rewritten

$$v_1 = K\frac{\frac{1}{2}C_T\Omega R}{(\mu^2+\lambda^2)^{\frac{1}{2}}}\frac{r}{R}\cos\psi \tag{13–2}$$

and

$$V\sin\alpha - v' = \lambda\Omega R - \lambda_1\Omega r\cos\psi \tag{13–3}$$

where

$$\lambda_1 = \frac{\frac{1}{2}KC_T}{(\mu^2+\lambda^2)^{\frac{1}{2}}} \tag{13–4}$$

$$v^1 = \text{resultant induced velocity} = v + v_1$$

Equation (7–4) is unchanged except in the cos ψ term, which becomes

$$\left(-\mu\Omega Ra_0 + \Omega rb_1 + \frac{1}{2}\mu\Omega Ra_2 - \lambda_1\Omega r\right)\cos\psi$$

Examination of equation (8–12) establishes that the net thrust is unaltered by λ_1, although the variation of the thrust with ψ is affected.

The increment in the thrust moment is obtained as

$$\Delta M_T = -\int_0^{BR}\frac{1}{2}\rho ca(\Omega r + \mu\Omega R\sin\psi)\lambda_1\Omega r\cos\psi r dr \tag{13–5}$$

which yields upon integration

$$\Delta M_T = \frac{1}{2}\rho ca\Omega^2R^4\left\{-\frac{1}{4}\lambda_1B^4\cos\psi - \frac{1}{6}\mu\lambda_1B^3\sin 2\psi\right\} \tag{13–6}$$

The small terms resulting from the second integral in (9–2) are ignored as being negligible. Referring to (9–11), it can be shown that the following changes are necessary in the expressions for b_1, a_2, and b_2:

$$\Delta b_1 = \frac{\lambda_1B^2}{B^2+\frac{1}{2}\mu^2} \tag{13–7}$$

$$\Delta a_2 = \frac{-\frac{1}{3}\mu\gamma^2\lambda_1B^7}{144+\gamma^2B^8} \tag{13–8}$$

$$\Delta b_2 = \frac{-4\mu\gamma\lambda_1B^3}{144+\gamma^2B^8} \tag{13–9}$$

The influence of λ_1 on the torque of the rotor is expressed in the following terms which are to be added to equation (10–4):

$$\frac{1}{8}\lambda_1^2B^4 + \frac{1}{3}\mu\lambda_1a_0B^3 - \frac{1}{4}\lambda_1b_1B^4 - \frac{1}{6}\mu\lambda_1a_2B^3 - \frac{8}{45\pi}a_0\lambda_1\mu^4 - \frac{1}{64}\lambda_1^2\mu^4 \tag{13–10}$$

The application of these results shows that for reasonable values of K the magnitude of the terms in (13–10) is such that the torque may be assumed unchanged by λ_1.

14. Vertical descent.—The analysis of existing data and the application of the previous development to the high-angle-of-attack operation of the autogiro have shown that the strip analysis is not valid in that range. The following treatment is based upon an analysis of data obtained from tests of propellers of low pitch, and given in detail in reference 5. The essential part of the reference is reproduced in figure 4 of this report, which shows the two quantities $\frac{1}{F}$ and $\frac{1}{f}$ as functions of each other. The symbols F and f represent the thrust coefficients of a propeller based respectively upon the velocity at the propeller disk and the velocity of flow at infinity. That is

$$F = \frac{T}{2\pi R^2\rho V_0^2} \tag{14–1}$$

$$f = \frac{T}{2\pi R^2\rho V^2} \tag{14–2}$$

where V_0 is the velocity at the propeller disk and for the autogiro is equal to $\lambda\Omega R$.

In the application of figure 4 to the autogiro, it can be stated that the rotor operates always on the branch of the curve in figure 4 labeled "windmill decelerating state", which is defined as that condition of operation in which the thrust of a propeller is in the direction considered as normal, while the propeller is moving in a direction opposite to the one considered normal and rotating in a positive sense.

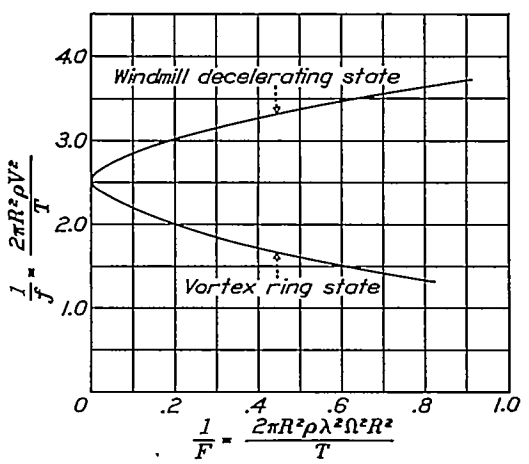

FIGURE 4.—Relation between propeller thrust coefficients based respectively upon velocity of translation and velocity at propeller disk.

In order to calculate the drag coefficient of a rotor at 90° angle of attack, the factor λ is calculated from equation (10–4) for $\mu=0$; C_T is then found from equation (8–14). From (14–1),

$$\frac{1}{F} = \frac{2\lambda^2}{C_T} \tag{14–3}$$

The value of $\frac{1}{f}$ corresponding to the calculated value of $\frac{1}{F}$ is then obtained from figure 4. From (3–3) and (14–2)

$$C_{D_r}' = \frac{4}{\frac{1}{f}} \tag{14–4}$$

where C_{D_r}' is the drag coefficient of the rotor at 90° angle of attack.

The vertical velocity and rotor speed are easily determined from the drag coefficient of the rotor and the rotor loading in pounds per square foot of disk area.

15. Application of analysis.—The lift, drag, angle of attack, blade motion, and rotor center of pressure of any rotor of given geometric form may be calculated from the equations developed in the previous analysis by a relatively simple series of operations. It is necessary that the following data be known: Pitch angle θ and the characteristic of its variation with the radius; solidity σ; mass constant of the blade γ; and the lift-curve slope and minimum drag coefficient of the blade airfoil section. The operations, in order, by which the aerodynamic characteristics of the rotor are calculated are as follows:

(*a*) Substitute the physical characteristics of the rotor in equations (9–11) and (9–15) and obtain the coefficients a_0, a_1, b_1, a_2, and b_2 as functions of μ and λ only.

(*b*) Substitute the functions from (a) in equation (10–4) and, choosing a suitable series of values for μ, solve (10–4) for λ as a function of μ.

(*c*) Substitute the rotor constants and λ in equation (8–14) and obtain C_T as a function of μ.

(*d*) Substitute for λ in equation (5–2) and obtain α as a function of μ.

(*e*) Substitute for λ in equations (9–11) and (9–15) and obtain a_0, a_1, b_1, a_2, and b_2 as functions of μ.

(*f*) Assign a value to K and obtain λ_1.

(*g*) Determine influence of (13–10) on λ as a function of μ.

(*h*) Evaluate (13–7), (13–8), and (13–9) and determine the changes in b_1, a_2, and b_2 arising from λ_1.

(*i*) Substitute for C_T in equation (11–4) and obtain D/L as a function of μ.

(*j*) Determine C_{L_r} from equation (3–6), and C_{D_r} from equations (11–4) and (3–6).

(*k*)Determine the rotor pitching and rolling moments from the appropriate equations in section 12.

(*l*) Determine $\frac{1}{F}$ from equation (14–1) for values of λ and C_T at μ equal to zero.

(*m*) Obtain $\frac{1}{f}$ from figure 4, and C_{D_r}' from equation (14–2).

In the numerical application of the analysis, arbitrary values must be assigned to several of the parameters in the equations. When an allowance is made for tip losses it appears reasonable to give to B a value which when multiplied by the radius will result in the radius less one-half the chord at the tip, although for blades that differ materially from the rectangular plan form assumed in the analysis, judgment must be used in applying such a rule. The slope of the lift curve should be that corresponding to infinite aspect ratio, and the value of 5.85 is suggested as a good average for most airfoils. The average drag coefficient, as has been previously stated, should be given a value one and one-half times the minimum drag coefficient of the airfoil section.

It is pertinent to mention at this time that the case analyzed in this paper is confined to blades of constant chord and section. The analysis of blades that do not conform to this limitation presents no difficulty, however, since an appropriate function of the radius can be substituted for c and/or δ before integrating the basic expressions with respect to the radius.

EXPERIMENTAL AND CALCULATED ROTOR CHARACTERISTICS

Scope of study.—The validity of the analysis presented in the first part of this paper is here examined by comparing experimental and calculated values of the different rotor characteristics. Relatively complete full-scale data are available on the characteristics of a Pitcairn PCA–2 autogiro (references 3 and 4). The physical constants of the PCA–2 rotor were determined and used to calculate the rotor characteristics by the equations previously developed; the results were then compared with measured values of the same quantities.

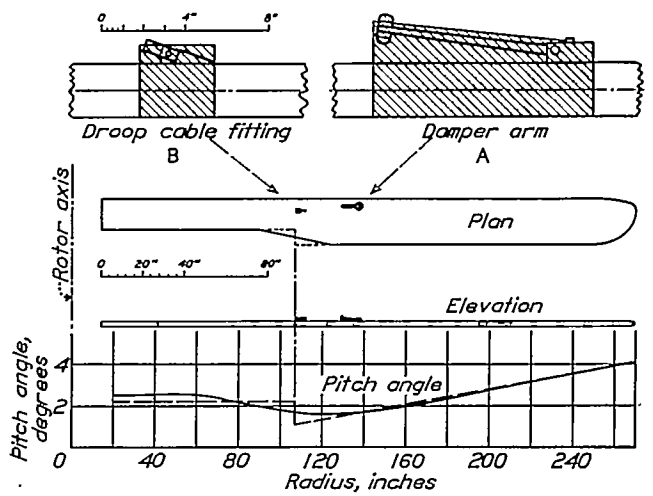

FIGURE 5.—Plan form, pitch angle, and protuberances of PCA–2 autogiro blade.

Physical constants of PCA–2 rotor.—The physical constants of the PCA–2 rotor are listed below:

Number of blades	4.
Blade radius	22.5 ft.
Blade airfoil section	Göttingen 429.
Blade moment of inertia about flapping hinge	334 slug ft.^{2}
From 0 to 39.4 percent R:	
Blade chord	1.25 ft.
Pitch angle	0.0384 rad.
From 39.4 to 100 percent R:	
Blade chord	1.833 ft.
Pitch angle	$-0.0157+0.0872\frac{r}{R}$ rad.

The pitch angle of the blade as measured in flight is plotted in figure 5 with a drawing of the plan and elevation of the blade. The dashed lines in figure 5

show the plan form and pitch angle as expressed by the foregoing constants; the blade was considered in two steps. The measurement of the pitch angle in flight is mandatory for the reason that the blade lift is offset from the center of gravity of the blade and causes a torsional deflection in flight which in this case amounts to approximately 2.4° (0.0419 radian) at the tip. The blade moment of inertia was determined by a swinging test in which particular care was taken to eliminate the virtual-mass effects of the ambient air; the above-mentioned value was obtained by two independent methods which reduced the virtual-mass effects to a minimum.

Attention is called to the fittings A and B shown in figure 5, the damper arm for interblade bracing and the droop-cable fitting. Since protuberances on the upper surface of an airfoil may cause serious increases in the drag of the airfoil, the qualitative influence of these fittings upon the rotor characteristics is subsequently examined.

The remaining constants required for the calculation of the rotor characteristics were chosen in accordance with the discussion in section 15 of the analysis; they are

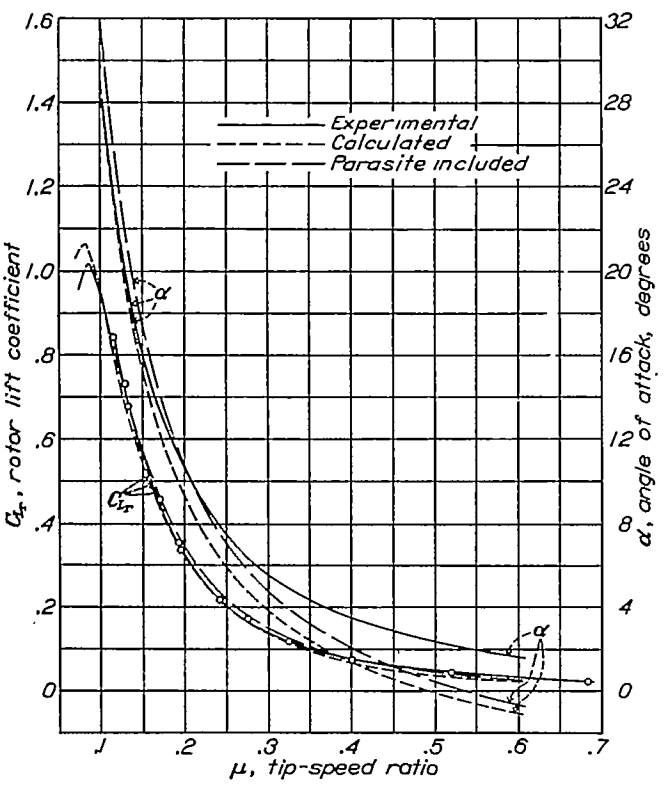

FIGURE 6.—Experimental and calculated lift coefficient and angle of attack of PCA-2 autogiro rotor, with calculated influence of estimated blade parasite drag.

B	0.959.
a	5.85.
δ	0.0120.
σ	0.1038.
W	3,000 lb.
ρ	0.00210 slug/cu.ft.

The solidity σ of the rotor was calculated from equation (8–13); the blade chord used was that of the outer straight portion. No serious error would be introduced in the calculations if the decrease in chord of the inner portion of the blade were ignored. The density given corresponds to the average density encountered during the tests reported in references 3 and 4, so that any but minor corrections to the experimental curve of rotor speed as a function of tip speed could be avoided.

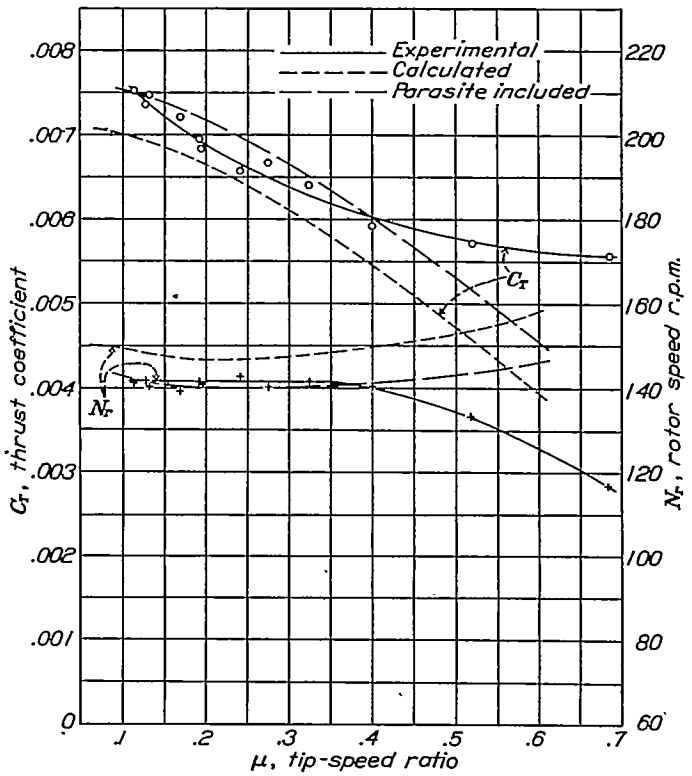

FIGURE 7.—Experimental and calculated thrust coefficient and rotor speed of PCA-2 autogiro rotor, with calculated influence of estimated blade parasite drag.

Results of analysis.—The blade plan form of the PCA-2 rotor requires an alteration of the equations for the rotor characteristics to take account of the change in chord. This alteration is accomplished by performing the integration from 0 to R in two steps, one from 0 to 39.4 percent R, the other from 39.4 to 100 percent R, using the proper value for the chord in each step. The resultant equations are similar in form to the ones derived for the case of constant chord, the difference being only in the numerical factors by which the several terms are multiplied.

The calculated characteristics of the PCA-2 rotor are presented in figures 6, 7, and 8, the experimental values being plotted in the same figures for comparison. These figures show the results of calculations that neglected the influence of the parasite drag added by the protuberances on the blade and assumed an induced flow constant in magnitude over the rotor disk. Rotor speed was calculated from the load curve shown in figure 9, which is reproduced from reference 4. It should be noted that the curve of experimental angle

of attack shown in figure 6 is taken from reference 3, as direct measurements were made of the angle of attack in those tests, whereas the measurements made in reference 4 required that the angle be calculated from the measured vertical velocities.

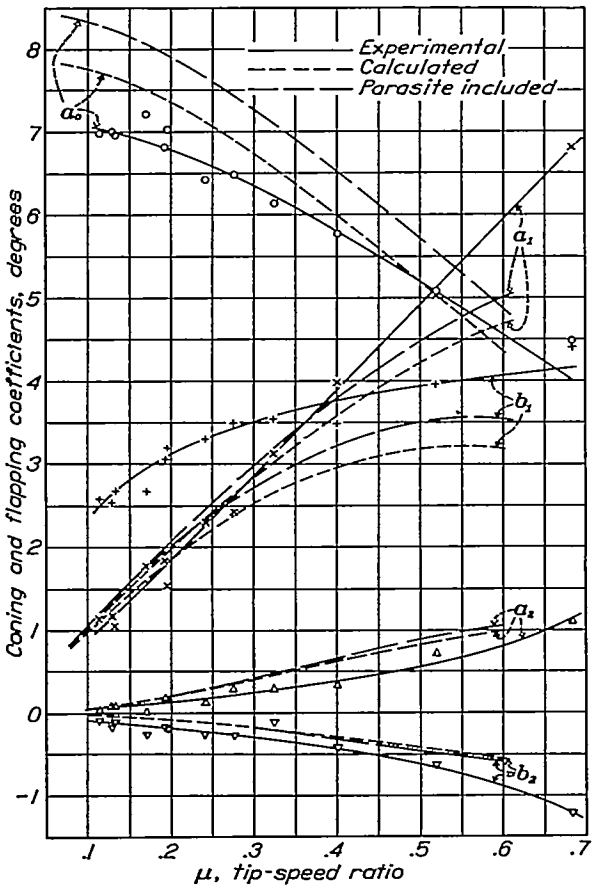

FIGURE 8.—Experimental and calculated blade motion coefficients of PCA-2 autogiro rotor, with calculated influence of estimated blade parasite drag.

The influence on the rotor characteristics of the protuberances on the blades was determined qualitatively by assuming that the flow was spoiled over that portion of the blade immediately behind the protuberance, which was assumed to result in a drag coefficient

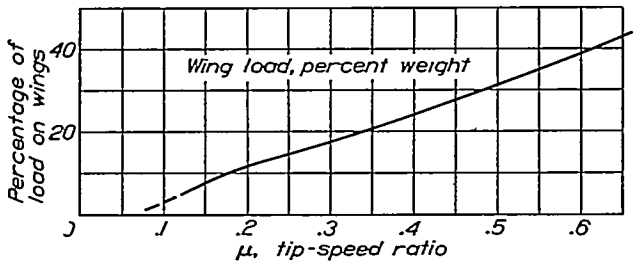

FIGURE 9.—Load carried by fixed wing of PCA-2 autogiro as a function of tip-speed ratio.

of unity for the cross-hatched portions of the frontal area of the blade shown in figure 5. The added drag was computed both as additional torque, which influenced the parameter λ, and as an added source of energy loss, which changed the expression for the lift-drag ratio. The results of these calculations are also shown in figures 6, 7, and 8 for comparison with both the experimental data and the original calculations.

The effect on the blade-motion coefficients of a nonuniform induced velocity of the type previously analyzed is shown in figure 10, in which experimental results and the original calculations are also plotted. Since this type of flow does not alter the force coefficients the remainder of the rotor characteristics have not been shown. These calculations are based arbitrarily on a constant value for K of 0.5 (see equation (13–4)), which may be too large at very low tip-speed ratios. The resultant motion of a blade, shown as a graph of β against ψ, is plotted in figure 11; experimental and calculated values are presented for a tip-speed ratio of 0.50.

The calculated rotor characteristics showing the combined effect of allowing for the additional drag of the protuberances on the blade, and the nonuniform induced velocity, are shown in figures 12, 13, and 14, for comparison with experimental values. The con-

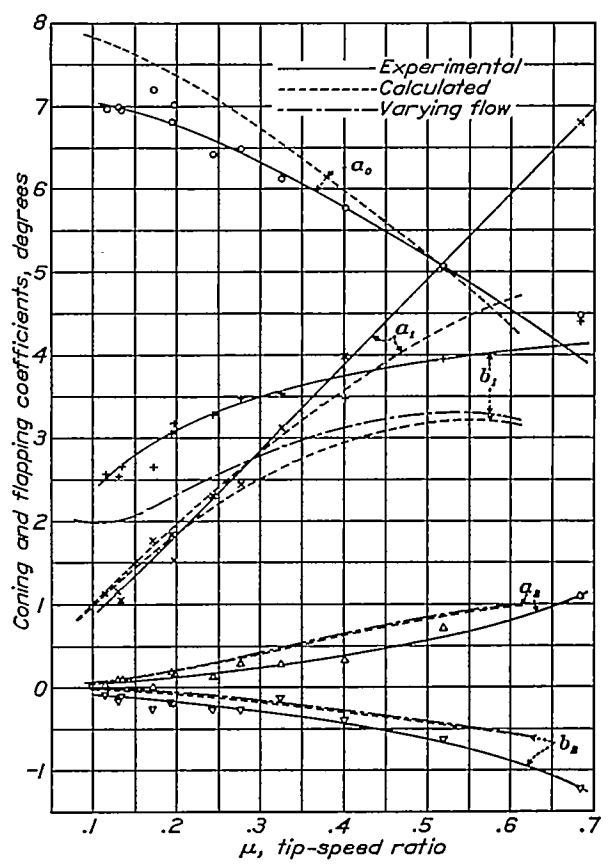

FIGURE 10.—Experimental and calculated blade motion coefficients of PCA-2 autogiro rotor, with calculated influence of assumed type of varying induced flow.

stants used in computing the combined influence of the two quantities are the same as those previously given.

The computation of the rotor drag coefficient at 90° angle of attack is shown in the following table for both the original computation and the computation

including the blade-parasite drag. Experimental values of the drag coefficient were calculated from the results in reference 3 by assuming that the fixed wing supported a portion of the weight corresponding to a normal-force coefficient of unity.

ROTOR CHARACTERISTICS AT 90° ANGLE OF ATTACK

	Original calculations	Parasite included	Experimental results
μ	0	0	----------
λ	.0218	.0256	----------
C_T	.00718	.00767	0.00666
CD_r'	1.370	1.343	1.222
Ω, rad./sec	15.44	14.96	15.04
$V_{v_{ind}}$, f.p.s	33.3	33.6	35.4

DISCUSSION

Method of analysis.—The most uncertain assumption made in the analysis is that the induced downward velocity generated by the rotor is constant in value over the rotor disk and equals the induced velocity of an airfoil of equal span and total load. The constant-valued part of the assumption is undoubtedly untrue, especially at low tip-speed ratios when the rotor loading is practically zero near the axis of rotation. At high tip-speed ratios the induced velocity probably approaches the constant value, insofar as variations along the span are concerned, but here also it is to be expected that variations in magnitude will occur over the disk, since the induced velocity probably changes along the chord. It has been partly demonstrated, however, that variations in the distribution of the induced velocity have a negligible influence on the net rotor forces, although they have a pronounced influence on the blade motion. The importance of these variations of the induced velocity may then be considered small. The assumption that the rotor is equivalent to an airfoil determines the virtual mass of air influenced by the rotor forces.

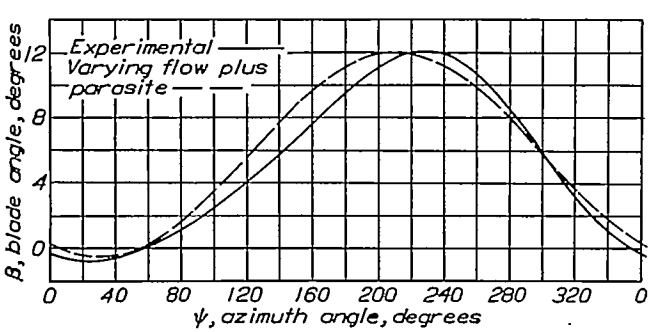

FIGURE 11.—Experimental and calculated blade motion of the PCA-2 autogiro rotor. μ=0.50.

This assumption is probably least in error at high tip-speed ratios where the rotor loading projected on the span axis approaches that obtained with an airfoil. The failure of the strip analysis at high angles of attack, that is, at low tip-speed ratios, can probably be traced to this assumption, which undoubtedly introduces an appreciable error as the operation of the rotor becomes closely similar to that of a windmill operating under conditions of axial flow.

Quantitative errors introduced by assuming that the angles φ and β are equal to their sines and that the cosines are equal to unity are believed to be negligible.

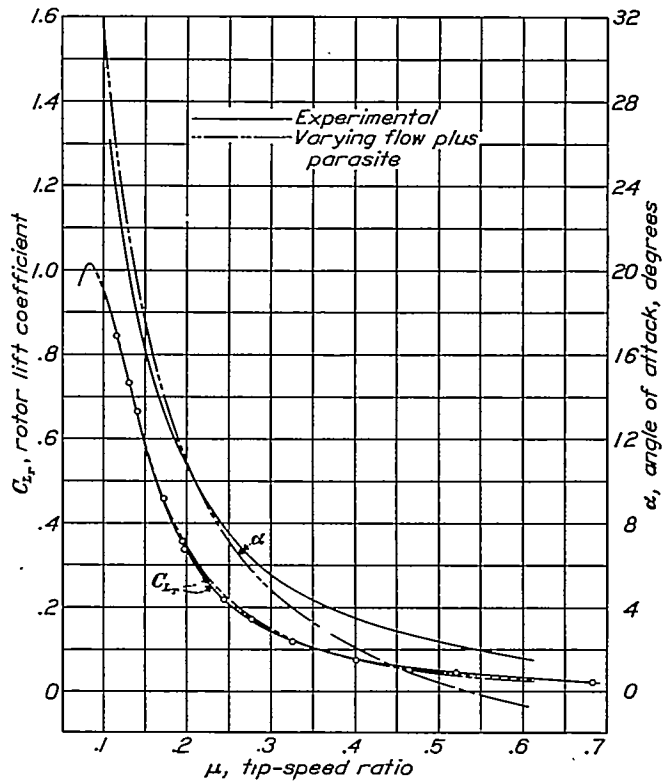

FIGURE 12. Experimental and calculated lift coefficient and angle of attack of PCA-2 autogiro rotor, including the calculated influence of both blade parasite drag and varying induced flow.

The angle φ becomes large only in regions of low resultant velocity where the air forces practically vanish in comparison with the forces developed in the high-velocity regions. The angle β does not exceed 15° and the error between the angle and its sine at that value is 1 percent; between the cosine and unity, 3 percent.

The neglect of the radial velocity in computing profile-drag power losses introduces an error of uncertain magnitude in the drag coefficients. This error is combined with the errors introduced by the use of an average drag coefficient for the blade elements and the approximate consideration of the blade parasite drag. Because of the impossibility of measuring rotor drag in flight, no analysis even of the combined errors can now be made.

Results.—Figures 6, 7, and 8, showing the comparison between experimental results and original calculations and the calculations which include the approximate influence of the blade parasite drag, demonstrate the varying agreement between the different characteristics. In figure 6 it is seen that the calculated rotor lift coefficient is in both cases in excellent agreement with experimental results. Calculated angle of attack, however, is appreciably in error and especially at high

tip-speed ratios, although the error in the original calculations is reduced by considering the blade parasite drag. In figure 7 the errors in the calculated thrust coefficient and rotor speed at high tip-speed ratios are clearly demonstrated, the errors becoming important above a tip-speed ratio of about 0.40. As in the pre-

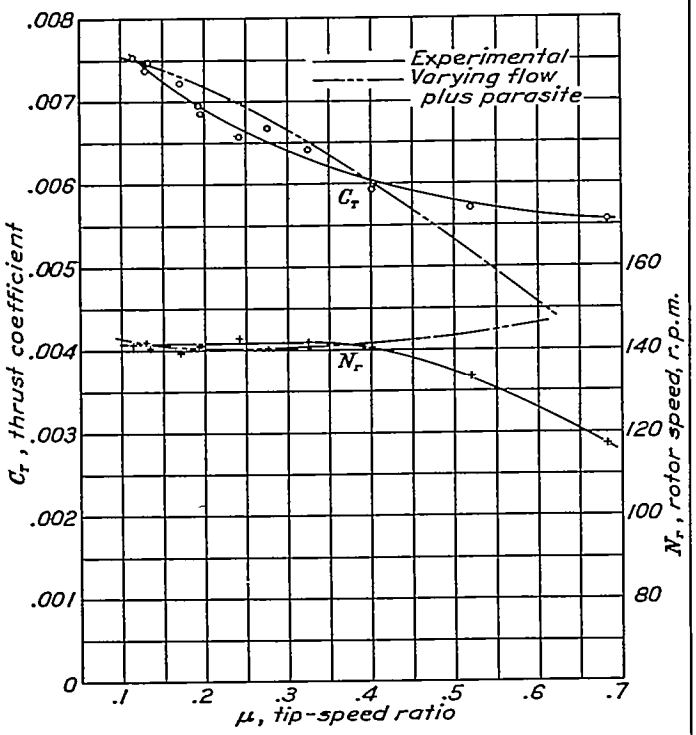

FIGURE 13.—Experimental and calculated thrust coefficient and rotor speed of PCA-2 autogiro rotor, including the calculated influence of both blade parasite drag and varying induced flow.

vious figure, the consideration of the blade parasite drag resulted in closer agreement between calculation and experiment. Figure 8 shows that the blade motion is, of all the characteristics, the least susceptible to calculation. The coefficient a_0 is in error at low tip-speed ratios, although the error decreases as the tip-speed ratio increases. The coefficient a_1 diverges more and more from experimental values as the tip-speed ratio approaches a maximum. The coefficient b_1, on the other hand, shows the greatest errors at low tip-speed ratios. The absolute magnitude of the errors in a_2 and b_2 is small, but the percentage is large. Figure 10 demonstrates that the calculated value of b_1 depends critically upon the variation of the induced velocity along the chord of the rotor disk. The influence of this variation on a_2 and b_2 is relatively unimportant.

Summing up the final results as shown in figures 12, 13, and 14, it can be stated that the calculated lift coefficient is in satisfactory agreement with the experimental over the entire range; the angle of attack is appreciably in error at large tip-speed ratios; the thrust coefficient and rotor speed show large errors, but only at high tip-speed ratios; and the blade motion shows an almost general unsatisfactory agreement.

The discrepancy in a_0 shown in figure 14 is probably due to the fact that the induced velocity in reality increases near the tip of the blade, whereas it is assumed constant. This disagreement means either that the calculated center of thrust occurs at too large a radius, or that an insufficient allowance has been made for the tip losses. The discrepancy in a_1 at high tip-speed ratios can probably be traced to the same error in basic assumption. The errors in b_1, a_2, and b_2 could probably be materially decreased by a proper choice of the constant determining the parameter λ_1 in equation (13–4). There is a possibility also that equation (13–2) should include a sine term at high tip-speed ratios where the difference in operation of the two halves of the rotor disk on opposite sides of the plane of symmetry is most pronounced. This additional term involving sin ψ would influence the thrust coefficient C_T and the blade-motion coefficient a_1 and would probably reduce the discrepancy obtained in both of them.

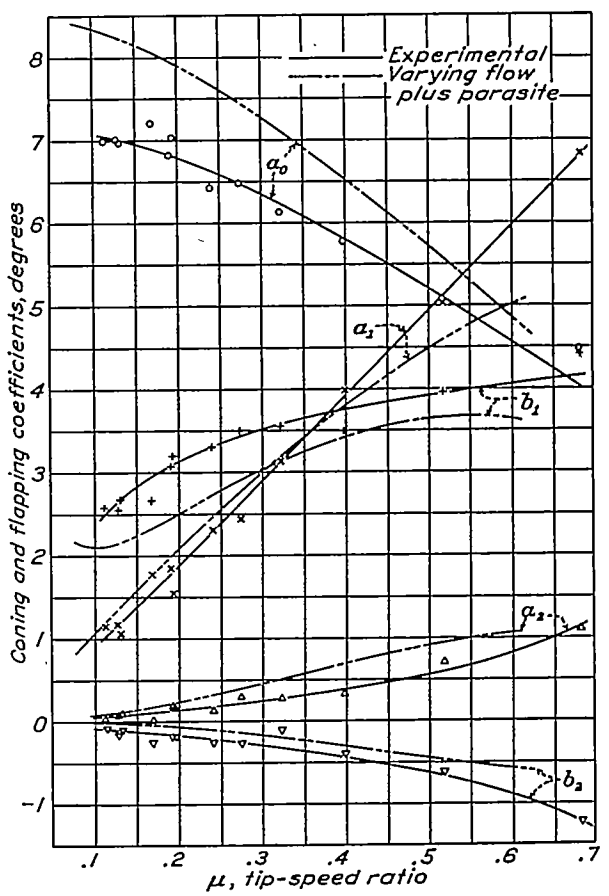

FIGURE 14.—Experimental and calculated blade motion coefficients of PCA-2 autogiro rotor, including the calculated influence of both blade parasite drag and varying induced flow.

The calculated drag coefficient at high incidence is 1.343, which is reasonably close to the value of 1.222 obtained from reference 3 by assuming that at 90° angle of attack the rotor carries the entire weight less a wing load corresponding to a drag coefficient of unity.

The vertical velocity calculated from this drag coefficient is 33.6 feet per second, which compares favorably with the experimental value of 35.4 feet per second. The calculated rotor speed is 14.96 radians per second compared to the experimental value of 15.04 radians per second.

The results of the analysis demonstrate the practicability and, in most respects, the usable accuracy of the strip analysis outlined in section 1. It is unfortunate that the experimental rotor drag cannot, at the present time, be presented for comparison with the calculated drag since, for the prediction of performance, this quantity is the most important rotor characteristic. It is, however, planned to test a PCA-2 rotor in the N.A.C.A. full-scale wind tunnel in the near future in order to obtain information for a detailed and thorough analysis of the rotor drag.

CONCLUSIONS

1. The aerodynamic analysis of the autogiro as developed by Glauert and Lock is quantitatively usable except for the blade motion.

2. The blade motion is critically dependent upon the distribution of induced velocities over the rotor disk and cannot be calculated rigorously without the accurate determination of the induced flow.

3. The analysis indicates that the type of induced flow assumed has only a secondary effect on the net rotor forces.

4. The parasite drag of the rotor blades is an important factor in the calculation of rotor characteristics.

Langley Memorial Aeronautical Laboratory,
National Advisory Committee for Aeronautics,
Langley Field, Va., *January 17, 1934.*

REFERENCES

1. Glauert, H.: A General Theory of the Autogyro. R. & M. No. 1111, British A.R.C., 1926.
2. Lock, C. N. H.: Further Development of Autogyro Theory—Parts I and II. R. & M. No. 1127, British A.R.C., 1928.
3. Wheatley, John B.: Lift and Drag Characteristics and Gliding Performance of an Autogiro as Determined in Flight. T.R. No. 434, N.A.C.A., 1932.
4. Wheatley, John B.: Wing Pressure Distribution and Rotor-Blade Motion of an Autogiro as Determined in Flight. T.R. No. 475, N.A.C.A., 1933.
5. Lock, C. N. H., Bateman, H., and Townend, H. C. H.: An Extension of the Vortex Theory of Airscrews with Applications to Airscrews of Small Pitch, Including Experimental Results. R. & M. No. 1014, British A.R.C., 1926.